2018

The influence of the N-terminal region proximal to the core domain on the assembly and chaperone activity of αB-crystallin

Blagojce Jovcevski
University of Wollongong, bj611@uowmail.edu.au

John Andrew Aquilina
University of Wollongong, aquilina@uow.edu.au

Justin Benesch
University of Oxford

Heath Ecroyd
University of Wollongong, heathe@uow.edu.au

Publication Details

Jovcevski, B., Aquilina, J., Benesch, J. L. P. & Ecroyd, H. (2018). The influence of the N-terminal region proximal to the core domain on the assembly and chaperone activity of αB-crystallin. Cell Stress and Chaperones, 23 (5), 827-836.

The influence of the N-terminal region proximal to the core domain on the assembly and chaperone activity of αB-crystallin

Abstract
αB-Crystallin (HSPB5) is a small heat-shock protein that is composed of dimers that then assemble into a polydisperse ensemble of oligomers. Oligomerisation is mediated by heterologous interactions between the C-terminal tail of one dimer and the core "α-crystallin" domain of another and stabilised by interactions made by the N-terminal region. Comparatively little is known about the latter contribution, but previous studies have suggested that residues in the region 54-60 form contacts that stabilise the assembly. We have generated mutations in this region (P58A, S59A, S59K, R56S/S59R and an inversion of residues 54-60) to examine their impact on oligomerisation and chaperone activity in vitro. By using native mass spectrometry, we found that all the αB-crystallin mutants were assembly competent, populating similar oligomeric distributions to wild-type, ranging from 16-mers to 30-mers. However, circular dichroism spectroscopy, intrinsic tryptophan and bis-ANS fluorescence studies demonstrated that the secondary structure differs to wild type, the 54-60 inversion mutation having the greatest impact. All the mutants exhibited a dramatic decrease in exposed hydrophobicity. We also found that the mutants in general were equally active as the wild-type protein in inhibiting the amorphous aggregation of insulin and seeded amyloid fibrillation of α-synuclein in vitro, except for the 54-60 inversion mutant, which was significantly less effective at inhibiting insulin aggregation. Our data indicate that alterations in the part of the N-terminal region proximal to the core domain do not drastically affect the oligomerisation of αB-crystallin, reinforcing the robustness of αB-crystallin in functioning as a molecular chaperone.

Disciplines
Medicine and Health Sciences

Publication Details
Jovcevski, B., Aquilina, J., Benesch, J. L. P. & Ecroyd, H. (2018). The influence of the N-terminal region proximal to the core domain on the assembly and chaperone activity of αB-crystallin. Cell Stress and Chaperones, 23 (5), 827-836.

The influence of the N-terminal region proximal to the core domain on the assembly and chaperone activity of αB-crystallin

Blagojce Jovcevski[1], J. Andrew Aquilina[1], Justin L. P. Benesch[2] and Heath Ecroyd[1†]

[1]*Illawarra Health and Medical Research Institute and School of Biological Sciences, University of Wollongong, Northfields Ave, Wollongong, New South Wales 2522, Australia*

[2]*Department of Chemistry, Physical and Theoretical Chemistry Laboratory, South Parks Road, Oxford OX1 3QZ, United Kingdom*

[†]Correspondence to: heathe@uow.edu.au, +61-2-4221-3443

ORCID

Blagojce Jovcevski: 0000-0001-7999-1385

Justin L.P. Benesch: 0000-0002-1507-3742

Heath Ecroyd: 0000-0001-7574-0044

Keywords

Proteostasis, molecular chaperone, small heat-shock protein, native mass spectrometry, protein aggregation, αB-crystallin, HSPB5, amyloid fibrils.

Abstract

αB-crystallin (HSPB5) is a small heat-shock protein that is composed of dimers that then assemble into a polydisperse ensemble of oligomers. Oligomerisation is mediated by heterologous interactions between the C-terminal tail of one dimer and the core "α-crystallin" domain of another, and stabilised by interactions made by the N-terminal region. Comparatively little is known about the latter contribution, but previous studies have suggested that residues in the region 54-60 form contacts that stabilise the assembly. We have generated mutations in this region (P58A, S59A, S59K, R56S/S59R and an inversion of residues 54-60) to examine their impact on oligomerisation and *in vitro* chaperone activity. By using native mass spectrometry, we found that all the αB-crystallin mutants were assembly competent, populating similar oligomeric distributions to wild-type, ranging from 16-mers to 30-mers. However, circular dichroism spectroscopy, intrinsic tryptophan and bis-ANS fluorescence studies demonstrated that the secondary structure differs to wild-type, the 54-60 inversion mutation having the greatest impact. All the mutants exhibited a dramatic decrease in exposed hydrophobicity. We also found that the mutants in general were equally active as the wild-type protein in inhibiting the amorphous aggregation of insulin and seeded amyloid fibrillation of α-synuclein *in vitro*, except for the 54-60 inversion mutant, which was significantly less effective at inhibiting insulin aggregation. Our data indicate that alterations in the part of the N-terminal region proximal to the core domain do not drastically affect the oligomerisation of αB-crystallin, reinforcing the robustness of αB-crystallin in functioning as a molecular chaperone.

Introduction

The molecular chaperone αB-crystallin (also known as HSBP5) is a systemically expressed vertebrate small heat-shock protein (sHsp) that exists as an ensemble of large, dynamic, polydisperse oligomers that undergo continual subunit-exchange (Boelens 2014; Delbecq and Klevit 2013; Haslbeck et al. 2016; Hochberg and Benesch 2014). In conjunction with other sHsps, such as Hsp27 (HSPB1) and Hsp20 (HSPB6), αB-crystallin is an important component of the protein quality control network in cells, where it acts as a molecular chaperone (Balch et al. 2008; Ecroyd 2015; Kampinga et al. 2015; McHaourab et al. 2009; Treweek et al. 2015). Numerous neurodegenerative diseases are associated with malfunction of this quality control network, including Alzheimer's disease and Parkinson's disease (Balch et al. 2008; Hartl et al. 2011; Yerbury et al. 2016). Mutations in αB-crystallin are also associated with desmin-related cardiomyopathies and cataracts in the lens (Andley 2009; Clark et al. 2012; Ecroyd and Carver 2009; Thornell and Aquilina 2015). Overall, these studies demonstrate that the chaperone function of αB-crystallin is a key contributor to the maintenance of protein homeostasis (proteostasis) in the cell.

αB-crystallin is made up of three key regions, a β-sheet rich core "α-crystallin" domain (αCD; residues 66-149), which dimerises and is conserved amongst sHsp family members and is flanked by unstructured N-terminal (NTR; residues 1-65) and C-terminal regions (CTR; residues 150-178) (Fig. 1a). The quaternary dynamics of αB-crystallin involves the exchange of monomers between oligomers (Hochberg and Benesch 2014), and is rate-limited by an interaction made between the CTR of one monomer with the αCD of another monomer in an adjacent dimer (Baldwin et al. 2011a; Baldwin et al. 2011c) (Fig. 1b). Several studies have shown how the CTR and, in particular, residues in and flanking the conserved IXI motif, impact on oligomeric assembly (Delbecq et al. 2012; Hilton et al. 2013) (Fig. 1b).

The NTR has also been shown to mediate contacts between αB-crystallin subunits via residues 58-61 (Jehle et al. 2010; Jehle et al. 2011) (Fig. 1b), with a construct lacking the NTR having reduced oligomeric stability (Laganowsky et al. 2010). Furthermore, structures of sHsps from prokaryotes and plants in which this region is (at least partially) resolved indicate it forms contacts between NTRs (Hanazono et al. 2013; McHaourab et al. 2012; van Montfort et al. 2001). This evidence has been used in efforts to model the oligomeric

assembly of αB-crystallin (Baldwin et al. 2011b; Braun et al. 2011; Jehle et al. 2010; Jehle et al. 2011; Peschek et al. 2013).

To gain further insight into the importance of these NTR interactions, we have examined the role of residues 54-60 in the NTR of αB-crystallin, which are proximal to the αCD. We generated a series of mutant forms of αB-crystallin in which we perturbed this region by introducing changes in localised charge (S59K), polarity (S59A), flexibility (S59A, R56S/S59R, Invert 54-60) and secondary structure (P58A to discourage formation of an α-helix) (Braun et al. 2011) and examined their impact on structure and function using a combination of biophysical methods, native mass spectrometry (MS) and *in vitro* aggregation assays. We found that these mutants did not significantly affect the ability of αB-crystallin to oligomerise, but did induce local structural changes. In addition, while most of these mutations did not impact noticeably on chaperone activity, inversion of the residues in this region caused a decrease in ability of the protein to inhibit insulin aggregation. We propose that this region of the NTR is not a major contributor to overall oligomer stability of αB-crystallin, but instead may play a unique role in the recognition and sequestration of amorphously aggregating proteins.

Methods

Protein expression and purification. The gene encoding human αB-crystallin (*HSPB5;* UniProt accession number P02511) was expressed in *Escherichia coli* BL21(DE3) using a plasmid kindly gifted by Dr. W. C. Boelens and Dr. W. W. de Jong, in which *HSPB5* was cloned into pET24d(+) (Novagen). The NTR mutants of αB-crystallin (P58A, S59A, S59K, R56S/S59R and Invert 54-60) (Fig. 1a) were generated by site-directed mutagenesis of the WT gene by GenScript (USA) and these constructs were sequenced to confirm they coded for the desired mutation. Expression and purification of each recombinant protein was performed as described previously (Aquilina et al. 2013; Horwitz et al. 1998).

Analytical size-exclusion chromatography (SEC). The average oligomeric size of αB-crystallin WT and NTR mutants was determined by analytical-SEC. Samples (50 µM) were loaded onto a Superdex 200 10/300 GL analytical-SEC (GE Healthcare), which had been equilibrated in either 50 mM phosphate buffer (PB; pH 7.4) or 200 mM ammonium acetate (NH_4OAc; pH 6.8) at a flow rate of 0.3 mL/min, at room temperature. The SEC column was calibrated using standards (Bio-Rad) containing bovine thyroglobulin (670 kDa), bovine γ-globulin (158 kDa), chicken ovalbumin (44 kDa) and horse myoglobin (17 kDa).

Native mass spectrometry (MS). MS was performed on a Synapt G1 HDMS (Waters) using a nanoelectrospray ionisation source. Instrument conditions and sample preparation for all MS analyses were performed as previously described (Aquilina et al. 2013). Oligomeric distributions were determined by calculating the relative abundance of oligomers as a percentage of all oligomers present for each mutant (Aquilina et al. 2003).

Far-UV Circular Dichroism (CD) Spectroscopy. CD measurements were acquired as previously described (Kulig and Ecroyd 2012) using a J810 Far UV spectropolarimeter (Jasco). All proteins were prepared to a final concentration of 10 µM in 10 mM PB (pH 7.4). CD spectra were accumulated from 6 scans and smoothed using an in-built Savitzky-Golay algorithm.

Dynamic light scattering (DLS). To determine the mean particle size (Z-average) and relative thermal stability of αB-crystallin in solution, DLS was performed. Proteins were prepared in 50 mM PB (pH 7.4) at 50 µM and incubated at 37 °C for 1 h prior to measurement. Samples were plated (100 µL) into 96-well microwell plates and analysed using a Zetasizer Auto Plate

Sampler system (Malvern). Thermal stability was assessed by using a temperature gradient with 2.5 °C increments within the range of 25 °C to 95 °C. The melting temperature of each mutant was defined as the temperature at which there was a 2-fold increase in the hydrodynamic diameter compared to that measured for the protein at 25 °C. Experiments were repeated twice, and data shown are representative from these two experiments.

Intrinsic tryptophan and bis-ANS fluorescence. Intrinsic tryptophan fluorescence was used to examine changes in the tertiary and quaternary structure of αB-crystallin (αB-crystallin contains two tryptophan residues; W9 and W60), and bis-ANS fluorescence was used to measure the relative level of exposed hydrophobic regions. Tryptophan fluorescence and bis-ANS fluorescence spectra were attained using a Cary Eclipse fluorescence spectrophotometer (Varian). Proteins were prepared to a final concentration of 10 μM in 50 mM PB (pH 7.4). Proteins were incubated at room temperature for 15 min prior to tryptophan fluorescence analysis. bis-ANS (final concentration 20 μM) was then added and the samples incubated for 3 min at room temperature prior to measurement of bis-ANS fluorescence. The excitation wavelength was set at 295 nm and 350 nm and emission wavelength was recorded from 300-400 nm and 400-600 nm for tryptophan fluorescence and bis-ANS studies, respectively. The slit widths for excitation and emission spectra were both set at 5 nm.

Aggregation assays. The chaperone activity of the NTR αB-crystallin mutants was assessed via thioflavin-T (ThT) fluorescence (amyloid fibril) or light-scattering (amorphous aggregation) assays, using sealed 384-microwell plates and a FLUOstar Optima plate reader (BMG Lab Technologies). Amorphous aggregation of insulin (100 μM), incubated at 37 °C in 50 mM PB (pH 7.4) was initiated by addition of DTT (20 mM). The αB-crystallin proteins were added at molar ratios of 1:1 and 1:0.75 (insulin:αB-crystallin). Aggregation was monitored by measuring the change in apparent absorbance due to light scattering at 340 nm.

To examine the ability of the NTR αB-crystallin mutants to prevent amyloid fibril formation a previously described (Buell et al. 2014) α-synuclein elongation assay was performed. The expression and purification of α-synuclein was performed as previously described (Grey et al. 2011; Hoyer et al. 2002). This assay measures the ability of chaperones to inhibit the elongation of α-synuclein fibrils using short, preformed α-synuclein seed fibril as seeds.

Fibril elongation was measured *in situ* by monitoring ThT binding. Chaperones were added at a molar ratio of 1:0.5 and 1:0.25 (α-synuclein:αB-crystallin) to the monomeric pool of α-synuclein (50 μM) in 50 mM PB (pH 7.4) containing 50 μM ThT. Samples were incubated for 60 min at 37 °C and then 10% w/w α-synuclein seed fibrils were added to each sample. The ThT fluorescence in each sample was monitored using a 440/490 nm excitation/emission filter set.

The relative ability of each chaperone to prevent aggregation was evaluated by comparing the apparent absorbance or ThT fluorescence at the conclusion of each assay, as previously described (Ecroyd and Carver 2008). All assays were performed at least three times and data are reported as mean ± SEM of these independent assays. Data were analysed by one-way ANOVA and Dunnett's multiple comparisons post-hoc test using Prism 5.0 (GraphPad) software.

Results

Oligomerisation of αB-crystallin is robust to mutations in residues 54-60 of the NTR.

In order to characterise the role of residues 54-60 in the NTR of αB-crystallin, we generated a series of point mutations (P58A, S59A, S59K, R56S/S59R) and one in which we inverted the sequence ("invert", i.e. 54-60→60-54) (Fig. 1a). All of these proteins expressed and purified as per wild-type (WT) αB-crystallin, and were soluble. To assess their oligomeric state, we used analytical-SEC and native MS. SEC revealed that the αB-crystallin mutants have a near identical elution profile compared to WT, in both phosphate and ammonium acetate buffers. In each case, the αB-crystallin mutants elute as a large broad peak indicative of a large polydisperse assembly, with oligomeric masses ranging from 200 – 700 kDa, however they elute later in phosphate (used in other structural studies and aggregation assays) compared to ammonium acetate (used in native MS experiments) buffer (Fig. 2). Previous studies have shown that minor differences in both pH and buffer composition can significantly change the quaternary dynamics of αB-crystallin, which may be responsible for the differences in elution times of the proteins between these two buffer systems (Hochberg and Benesch 2014).

Native mass spectra for all proteins were qualitatively similar, displaying a broad region of signal between 8,000 – 12,000 *m/z* (Fig. 3, left panels), which is typical of large polydisperse proteins, and consistent with previous data for WT αB-crystallin (Aquilina et al. 2004; Benesch et al. 2008). To obtain higher-resolution insight, we performed collision-induced dissociation (CID) which, under the conditions employed, strips highly charged monomeric subunits off the oligomers, and allows the identification and quantification of all individual oligomers present (Aquilina et al. 2003). In this way, we were able to extract the oligomeric distributions for each of the mutants (Fig. 3, right panels). All the NTR mutants displayed distributions that did not differ significantly from WT αB-crystallin, with oligomers ranging from 16-mers to 30-mers observed, and the 22-mer being the most abundant in all cases (Fig. 3, right panels).

NTR mutations confer changes in secondary and tertiary structure of αB-crystallin.

To examine the structure of the NTR on a more local level, we employed a range of biophysical techniques. We first used far-UV CD spectroscopy to probe the secondary structure of these NTR mutants, and found that most of the αB-crystallin mutants, except for S59A, exhibited changes in secondary structure compared to the WT, with a shift towards more β-sheet content and concomitant loss of turns, whereas the S59A mutant was near-identical to WT (Fig. 4a). The invert mutation led to a dramatic change in the secondary structure of αB-crystallin compared to the WT protein, resulting in a significant increase in α-helical secondary structure and concomitant loss of random coil (Fig. 4a).

In order to determine the relative thermal stability of these mutants, we measured the mean particle size (diameter; Z-average) as a function of temperature using DLS (Fig. 4b). The average size of the αB-crystallin mutants in solution began to increase dramatically at 60 °C (Fig. 4b). All the mutant αB-crystallin mutants had a greater rate of increase in the average particle size than WT αB-crystallin, such that, at 75 °C, the average diameter of particles formed by all the mutants exceeded 250 nm, compared to 150 nm for the WT (Fig. 4b). These data demonstrate that the mutants are less stable than WT αB-crystallin.

To interrogate the tertiary structure of the αB-crystallin mutants, we performed intrinsic tryptophan- and bis-ANS-fluorescence. The S59K and R56S/S59R mutants exhibited greater intrinsic fluorescence intensity compared to WT, but no observable shift in emission maximum (Fig. 4c), suggestive of an abatement of fluorescence quenching (particularly considering these mutations are immediately adjacent to W60). The other mutants had a similar intrinsic tryptophan fluorescence profile to the WT αB-crystallin, also with no observable shift in emission maximum (Fig. 4c). Interestingly, all αB-crystallin mutants showed a substantial decrease and red shift (≈10 nm shift from 488 nm to 499 nm) in the bis-ANS fluorescence emission maximum compared to WT αB-crystallin (Fig. 4d) indicative of a substantial decrease in exposed hydrophobicity of the αB-crystallin NTR mutants.

Chaperone activity of αB-crystallin is perturbed by inversion of residues 54-60 in the NTR.

We next investigated the influence of these structural changes on the ability of the αB-crystallin mutants to prevent amyloid fibril formation and amorphous aggregation *in vitro*. We used α-synuclein as a model protein for fibrillar aggregation and insulin for amorphous aggregation. Moreover, the aggregation of α-synuclein, an intrinsically disordered protein, has been extensively characterised (Buell et al. 2014; Wordehoff et al. 2017) and is associated with Parkinson's disease and dementia with Lewy bodies. In the absence of α-synuclein or insulin, no increase in ThT fluorescence or light scatter was observed (Fig. S1). In the absence of chaperone, α-synuclein seeds were observed to elongate through addition of monomeric α-synuclein such that, after ≈16 h, the change in ThT fluorescence associated with fibrillar aggregation had plateaued (Fig. 5a). In the presence of αB-crystallin, there was a decrease in ThT fluorescence indicative of the inhibition of α-synuclein fibril elongation. However, there was no significant difference in the ability of the αB-crystallin mutants to prevent seeded α-synuclein aggregation (Fig. 5a).

In the absence of chaperone, insulin was observed to aggregate rapidly upon reduction with DTT such that, after ≈15 min, the light scatter associated with its aggregation into large insoluble particles had plateaued (Fig. 5b). Whereas in the presence of αB-crystallin, there was a decrease in light scatter, indicative of insulin aggregation inhibition. There was no significant difference in the ability of the αB-crystallin mutants to prevent the amorphous aggregation of insulin, with the exception of the 54-60 invert mutant, which showed a significant decrease in ability to prevent insulin aggregation compared to WT αB-crystallin at both 1:1 and 1:0.75 molar ratios (insulin: αB-crystallin) (Fig. 5b). Taken together, these results suggest that modification of the 54-60 region of the NTR affects the activity of αB-crystallin to inhibit amorphous, but not fibrillar, aggregation.

Discussion

Here we have investigated the role of the region encompassing residues 54-60 in the NTR of αB-crystallin in relation to its structure and chaperone function. This region had previously been identified as making inter-dimer contacts (Braun et al. 2011; Jehle et al. 2011), and to affect the oligomerisation (Ghosh et al. 2006) and polydispersity (Sreelakshmi and Sharma 2006) of αB-crystallin. Our results reveal that mutations in this region do not drastically affect the oligomeric distribution populated by αB-crystallin. Instead, we found that mutation led to a reduction of random coil and, in particular for the invert mutant, an increase in α-helix. These changes in secondary structure were associated with decreases in exposed hydrophobicity and thermostability of the oligomers.

Our data demonstrates that residues 54-60 of the NTR are not necessary for oligomerisation, but rather stabilise the oligomeric forms that are mediated by associations between the CTR and the αCD. This is consistent with the observation that a construct of αB-crystallin, truncated of the NTR, is still assembly competent (Laganowsky et al. 2010). Similarly, deletion of the NTR has been shown not to abolish oligomeric assembly of archaeal sHsps (Shi et al. 2006; Usui et al. 2004) and deletion of residues 61-70 (analogous to 51-60 in αB-crystallin) in the NTR of Hsp20 (HSPB6) does not induce drastic changes to the structure and chaperone function compared to the WT protein (Heirbaut et al. 2014; Heirbaut et al. 2017). Moreover, the NTR is the location for the major phosphorylation sites of vertebrate sHsps, including αB-crystallin and Hsp27, whereby modification promotes the dissociation of oligomers (Jovcevski et al. 2015; McDonald et al. 2012; Peschek et al. 2013). It therefore appears that the role of the NTR in assembly is secondary to the CTR and the αCD, providing a means for regulating the oligomerisation of sHsps.

Our *in vitro* aggregation assays revealed that, in almost all cases, the αB-crystallin mutants were able to prevent amorphous aggregation of insulin and amyloid fibrillation of α-synuclein with comparable efficiency to WT. The exception was the invert mutant, which had a significantly reduced capacity to inhibit the amorphous aggregation of insulin. While these data did not readily correlate with differences in hydrophobicity, interestingly, the invert mutant was distinguished from the others by its different CD spectra, which suggested a shift in equilibrium from random coil structure to α-helix. This structural shift is compatible with the observation of heterogeneous αB-crystallin NTR conformations (Braun

et al. 2011; Jehle et al. 2011) and raises the possibility that changes in secondary structure in the NTR regulate interactions with aggregation-prone proteins. This hypothesis is consistent with data on archaeal sHsps, that shows a disorder to order transition (Takeda et al. 2011) and a propensity to form multiple helical configurations (Liu et al. 2015), particularly in its chaperone-active state.

Notably, while being less active in protecting against the aggregation of insulin, the invert mutant had a similar ability to prevent the amyloid formation of α-synuclein compared to WT αB-crystallin. This is suggestive of different regions of αB-crystallin being responsible for interacting with fibril-forming and amorphously aggregating proteins. Given that the mutation lies in the NTR, our data indicate that this region is important for the latter type of interaction, in line with chemical cross-linking data for interactions with different plant sHsps (Jaya et al. 2009; Lambert et al. 2013). Conversely, our data also suggests that the NTR is not the primary interaction site involved in inhibiting α-synuclein amyloid formation. This is also apparent with our previous data which showed that the isolated αCD is a potent inhibitor of amyloid formation, including that of α-synuclein (Cox et al. 2016; Hochberg et al. 2014). These observations add to emerging evidence that αB-crystallin forms differential interactions, depending on the morphology of aggregation-prone proteins (Kulig and Ecroyd 2012; Mainz et al. 2015).

In summary, our results suggest that residues 54-60 of the NTR have a subtle but discernible impact on the structure and chaperone function of αB-crystallin. The data align with the hypothesis that conformational changes in the NTR impact on inter-dimer contacts, as well as the interaction with aggregating proteins. However, the data also reflect the robust ability of αB-crystallin to oligomerise into polydisperse assemblies, despite significant changes in the lower levels of the structural hierarchy. This observation is line with the importance of αB-crystallin remaining oligomeric in the eye lens and thereby maintaining lens transparency (Tardieu 1998), despite the numerous post-translational modifications it accumulates over the life-time of the organism (Thornell and Aquilina 2015).

Author Contributions

B.J., J.A.A., J.L.P.B. and H.E. designed the research; B.J. performed the experiments; B.J., J.L.P.B., and H.E. analysed experimental data; B.J., J.L.P.B., and H.E. wrote the manuscript.

Acknowledgments

B.J. is supported by an Australian Rotary Health/The Henning Family matching Ph.D. scholarship. J.L.P.B. thanks the Biotechnology and Biological Science Research Council for support of this project (BB/J018082/1). H.E. was supported by an Australian Research Council (ARC) Future Fellowship (FT110100586). This research used equipment funded by ARC LIEF Grant (LE0882289) located at the UOW Mass Spectrometry User Resource and Research Facility (MSURRF). We would like to thank the Illawarra Health and Medical Research Institute and MSURRF for technical support.

References

Andley UP (2009) Effects of alpha-crystallin on lens cell function and cataract pathology Curr Mol Med 9:887-892 doi:https://www.ncbi.nlm.nih.gov/pubmed/19860667

Aquilina JA, Benesch JLP, Bateman OA, Slingsby C, Robinson CV (2003) Polydispersity of a mammalian chaperone: Mass spectrometry reveals the population of oligomers in alphab-crystallin Proceedings of the National Academy of Sciences of the United States of America 100:10611-10616 doi:10.1073/pnas.1932958100

Aquilina JA, Benesch JLP, Ding LL, Yaron O, Horwitz J, Robinson CV (2004) Phosphorylation of alphab-crystallin alters chaperone function through loss of dimeric substructure J Biol Chem 279:28675-28680 doi:10.1074/jbc.M403348200

Aquilina JA, Shrestha S, Morris AM, Ecroyd H (2013) Structural and functional aspects of hetero-oligomers formed by the small heat shock proteins alphab-crystallin and hsp27 J Biol Chem 288:13602-13609 doi:10.1074/jbc.M112.443812

Balch WE, Morimoto RI, Dillin A, Kelly JW (2008) Adapting proteostasis for disease intervention Science 319:916-919 doi:10.1126/science.1141448

Baldwin AJ, Hilton GR, Lioe H, Bagneris C, Benesch JLP, Kay LE (2011a) Quaternary dynamics of alphab-crystallin as a direct consequence of localised tertiary fluctuations in the c-terminus J Mol Biol 413:310-320 doi:10.1016/j.jmb.2011.07.017

Baldwin AJ, Lioe H, Hilton GR, Baker LA, Rubinstein JL, Kay LE, Benesch JLP (2011b) The polydispersity of alphab-crystallin is rationalized by an interconverting polyhedral architecture Structure 19:1855-1863 doi:10.1016/j.str.2011.09.015

Baldwin AJ, Lioe H, Robinson CV, Kay LE, Benesch JLP (2011c) Alphab-crystallin polydispersity is a consequence of unbiased quaternary dynamics J Mol Biol 413:297-309 doi:10.1016/j.jmb.2011.07.016

Benesch JLP, Ayoub M, Robinson CV, Aquilina JA (2008) Small heat shock protein activity is regulated by variable oligomeric substructure J Biol Chem 283:28513-28517 doi:10.1074/jbc.M804729200

Boelens WC (2014) Cell biological roles of alphab-crystallin Prog Biophys Mol Biol 115:3-10 doi:10.1016/j.pbiomolbio.2014.02.005

Braun N et al. (2011) Multiple molecular architectures of the eye lens chaperone alphab-crystallin elucidated by a triple hybrid approach Proc Natl Acad Sci U S A 108:20491-20496 doi:10.1073/pnas.1111014108

Buell AK et al. (2014) Solution conditions determine the relative importance of nucleation and growth processes in alpha-synuclein aggregation Proc Natl Acad Sci U S A 111:7671-7676 doi:10.1073/pnas.1315346111

Clark AR, Lubsen NH, Slingsby C (2012) Shsp in the eye lens: Crystallin mutations, cataract and proteostasis Int J Biochem Cell Biol 44:1687-1697 doi:10.1016/j.biocel.2012.02.015

Cox D, Selig E, Griffin MD, Carver JA, Ecroyd H (2016) Small heat shock proteins prevent alpha-synuclein aggregation via transient interactions and their efficacy is affected by the rate of aggregation The Journal of biological chemistry doi:10.1074/jbc.M116.739250

Delbecq SP, Jehle S, Klevit R (2012) Binding determinants of the small heat shock protein, alphab-crystallin: Recognition of the 'ixi' motif EMBO J 31:4587-4594 doi:10.1038/emboj.2012.318

Delbecq SP, Klevit RE (2013) One size does not fit all: The oligomeric states of alphab crystallin FEBS Lett 587:1073-1080 doi:10.1016/j.febslet.2013.01.021

Ecroyd H (2015) Redefining the chaperone mechanism of shsps: Not just holdase chaperones. The big book on small heat shock proteins. In: Tanguay RM, Hightower LE (eds) The Big Book on Small Heat Shock Proteins. Springer International Publishing, Cham, pp 179-195. doi: 10.1007/978-3-319-16077-1_7

Ecroyd H, Carver JA (2008) The effect of small molecules in modulating the chaperone activity of alphab-crystallin against ordered and disordered protein aggregation FEBS J 275:935-947 doi:10.1111/j.1742-4658.2008.06257.x

Ecroyd H, Carver JA (2009) Crystallin proteins and amyloid fibrils Cell Mol Life Sci 66:62-81 doi:10.1007/s00018-008-8327-4

Ghosh JG, Estrada MR, Clark JI (2006) Structure-based analysis of the beta8 interactive sequence of human alphab crystallin Biochemistry 45:9878-9886 doi:10.1021/bi060970k

Grey M, Linse S, Nilsson H, Brundin P, Sparr E (2011) Membrane interaction of alpha-synuclein in different aggregation states J Parkinsons Dis 1:359-371 doi:10.3233/JPD-2011-11067

Hanazono Y et al. (2013) Nonequivalence observed for the 16-meric structure of a small heat shock protein, sphsp16.0, from schizosaccharomyces pombe Structure 21:220-228 doi:10.1016/j.str.2012.11.015

Hartl FU, Bracher A, Hayer-Hartl M (2011) Molecular chaperones in protein folding and proteostasis Nature 475:324-332 doi:10.1038/nature10317

Haslbeck M, Peschek J, Buchner J, Weinkauf S (2016) Structure and function of alpha-crystallins: Traversing from in vitro to in vivo Biochim Biophys Acta 1860:149-166 doi:10.1016/j.bbagen.2015.06.008

Heirbaut M, Beelen S, Strelkov SV, Weeks SD (2014) Dissecting the functional role of the n-terminal domain of the human small heat shock protein hspb6 PLoS One 9:e105892 doi:10.1371/journal.pone.0105892

Heirbaut M, Lermyte F, Martin EM, Beelen S, Sobott F, Strelkov SV, Weeks SD (2017) Specific sequences in the n-terminal domain of human small heat-shock protein hspb6 dictate preferential hetero-oligomerization with the orthologue hspb1 J Biol Chem 292:9944-9957 doi:10.1074/jbc.M116.773515

Hilton GR, Hochberg GK, Laganowsky A, McGinnigle SI, Baldwin AJ, Benesch JLP (2013) C-terminal interactions mediate the quaternary dynamics of alphab-crystallin Philos Trans R Soc Lond B Biol Sci 368:20110405 doi:10.1098/rstb.2011.0405

Hochberg GK, Benesch JLP (2014) Dynamical structure of alphab-crystallin Prog Biophys Mol Biol 115:11-20 doi:10.1016/j.pbiomolbio.2014.03.003

Hochberg GK et al. (2014) The structured core domain of alphab-crystallin can prevent amyloid fibrillation and associated toxicity Proc Natl Acad Sci U S A 111:E1562-1570 doi:10.1073/pnas.1322673111

Horwitz J, Huang QL, Ding L, Bova MP (1998) Lens alpha-crystallin: Chaperone-like properties Methods in enzymology 290:365-383 doi:http://www.ncbi.nlm.nih.gov/pubmed/9534176

Hoyer W, Antony T, Cherny D, Heim G, Jovin TM, Subramaniam V (2002) Dependence of alpha-synuclein aggregate morphology on solution conditions Journal of Molecular Biology 322:383-393 doi:10.1016/S0022-2836(02)00775-1

Jaya N, Garcia V, Vierling E (2009) Substrate binding site flexibility of the small heat shock protein molecular chaperones Proc Natl Acad Sci U S A 106:15604-15609 doi:10.1073/pnas.0902177106

Jehle S et al. (2010) Solid-state nmr and saxs studies provide a structural basis for the activation of alphab-crystallin oligomers Nat Struct Mol Biol 17:1037-1042 doi:10.1038/nsmb.1891

Jehle S et al. (2009) Alphab-crystallin: A hybrid solid-state/solution-state nmr investigation reveals structural aspects of the heterogeneous oligomer J Mol Biol 385:1481-1497 doi:10.1016/j.jmb.2008.10.097

Jehle S et al. (2011) N-terminal domain of alphab-crystallin provides a conformational switch for multimerization and structural heterogeneity Proc Natl Acad Sci U S A 108:6409-6414 doi:10.1073/pnas.1014656108

Jovcevski B et al. (2015) Phosphomimics destabilize hsp27 oligomeric assemblies and enhance chaperone activity Chem Biol 22:186-195 doi:10.1016/j.chembiol.2015.01.001

Kampinga HH, de Boer R, Beerstra N (2015) The multicolored world of the human hspb family. In: Tanguay RM, Hightower LE (eds) The big book on small heat shock proteins. Springer International Publishing, Cham, pp 3-26. doi:10.1007/978-3-319-16077-1_1

Kulig M, Ecroyd H (2012) The small heat-shock protein alphab-crystallin uses different mechanisms of chaperone action to prevent the amorphous versus fibrillar aggregation of alpha-lactalbumin Biochem J 448:343-352 doi:10.1042/BJ20121187

Laganowsky A et al. (2010) Crystal structures of truncated alphaa and alphab crystallins reveal structural mechanisms of polydispersity important for eye lens function Protein Sci 19:1031-1043 doi:10.1002/pro.380

Lambert W, Rutsdottir G, Hussein R, Bernfur K, Kjellström S, Emanuelsson C (2013) Probing the transient interaction between the small heat-shock protein hsp21 and a model substrate protein using crosslinking mass spectrometry Cell Stress and Chaperones 18:75-85 doi:10.1007/s12192-012-0360-4

Liu L, Chen JY, Yang B, Wang FH, Wang YH, Yun CH (2015) Active-state structures of a small heat-shock protein revealed a molecular switch for chaperone function Structure 23:2066-2075 doi:10.1016/j.str.2015.08.015

Mainz A et al. (2015) The chaperone alphab-crystallin uses different interfaces to capture an amorphous and an amyloid client Nature structural & molecular biology 22:898-905 doi:10.1038/nsmb.3108

McDonald ET, Bortolus M, Koteiche HA, McHaourab HS (2012) Sequence, structure, and dynamic determinants of hsp27 (hspb1) equilibrium dissociation are encoded by the n-terminal domain Biochemistry 51:1257-1268 doi:10.1021/bi2017624

McHaourab HS, Godar JA, Stewart PL (2009) Structure and mechanism of protein stability sensors: Chaperone activity of small heat shock proteins Biochemistry 48:3828-3837 doi:10.1021/bi900212j

McHaourab HS, Lin YL, Spiller BW (2012) Crystal structure of an activated variant of small heat shock protein hsp16.5 Biochemistry 51:5105-5112 doi:10.1021/bi300525x

Peschek J et al. (2013) Regulated structural transitions unleash the chaperone activity of alphab-crystallin Proc Natl Acad Sci U S A 110:E3780-3789 doi:10.1073/pnas.1308898110

Shi J, Koteiche HA, McHaourab HS, Stewart PL (2006) Cryoelectron microscopy and epr analysis of engineered symmetric and polydisperse hsp16.5 assemblies reveals determinants of polydispersity and substrate binding J Biol Chem 281:40420-40428 doi:10.1074/jbc.M608322200

Sreelakshmi Y, Sharma KK (2006) The interaction between alphaa- and alphab-crystallin is sequence-specific Mol Vis 12:581-587 doi:https://www.ncbi.nlm.nih.gov/pubmed/16760894

Takeda K, Hayashi T, Abe T, Hirano Y, Hanazono Y, Yohda M, Miki K (2011) Dimer structure and conformational variability in the n-terminal region of an archaeal small heat shock protein, sthsp14.0 J Struct Biol 174:92-99 doi:10.1016/j.jsb.2010.12.006

Tardieu A (1998) Alpha-crystallin quaternary structure and interactive properties control eye lens transparency Int J Biol Macromol 22:211-217 doi:https://www.ncbi.nlm.nih.gov/pubmed/9650075

Thornell E, Aquilina A (2015) Regulation of alphaa- and alphab-crystallins via phosphorylation in cellular homeostasis Cell Mol Life Sci 72:4127-4137 doi:10.1007/s00018-015-1996-x

Treweek TM, Meehan S, Ecroyd H, Carver JA (2015) Small heat-shock proteins: Important players in regulating cellular proteostasis Cell Mol Life Sci 72:429-451 doi:10.1007/s00018-014-1754-5

Usui K, Hatipoglu OF, Ishii N, Yohda M (2004) Role of the n-terminal region of the crenarchaeal shsp, sthsp14.0, in thermal-induced disassembly of the complex and molecular chaperone activity Biochem Biophys Res Commun 315:113-118 doi:10.1016/j.bbrc.2004.01.031

van Montfort RL, Basha E, Friedrich KL, Slingsby C, Vierling E (2001) Crystal structure and assembly of a eukaryotic small heat shock protein Nat Struct Biol 8:1025-1030 doi:10.1038/nsb722

Wordehoff MM et al. (2017) Opposed effects of dityrosine formation in soluble and aggregated alpha-synuclein on fibril growth J Mol Biol doi:10.1016/j.jmb.2017.09.005

Yerbury JJ et al. (2016) Walking the tightrope: Proteostasis and neurodegenerative disease J Neurochem 137:489-505 doi:10.1111/jnc.13575

Figure Legends

Fig. 1: The NTR proximal to the αCD is involved in forming intra-dimer contacts in αB-crystallin. **a** The structured αCD (grey) which contains the heterogenous region 1 (HR1; *underlined*) (Jehle et al. 2009) is flanked by unstructured N-terminal (NTR, red) and C-terminal (CTR, green) regions. Several mutations were incorporated into αB-crystallin proximal to the αCD (residues 54-60) to investigate their impact on structure and function. **b** Previous solid-state NMR studies on αB-crystallin dimers (pdb entry: 2klr) (Jehle et al. 2010) implicate NTR residues 52-62 (β2a; red) in forming intra-dimer contacts with the β3-sheet, whilst the CTR (via. the IXI motif; residues 156-163; green) binds to the β4-8 groove in adjacent monomers to provide stability to αB-crystallin oligomers.

Fig. 2: Analytical-SEC shows no significant change in quaternary structure between αB-crystallin mutants. Analytical-SEC of NTR αB-crystallin mutants in 50 mM PB (pH 7.4) (*top panel*) and 200 mM ammonium acetate (NH_4OAc) (pH 6.8) (*bottom panel*) which illustrates the presence of large oligomers in solution. Elution volume of molecular weight standards are indicated above the chromatograms (in kDa).

Fig. 3: Native MS reveals no significant change in oligomeric distribution between αB-crystallin mutants. Spectra were acquired at both low (20 V; grey) and high (200 V; black) activation conditions (*left panels*) where signal in the overlapping *n-2* and *n-3* regions (13,000 – 30,000 *m/z*) were substantially resolved by the sequential dissociation of monomers from an oligomer (schematically illustrated above). The charge state distributions in this region were used to identify and determine the relative abundance of each αB-crystallin mutant. Oligomeric distributions of αB-crystallin mutants (*right panels*), with large oligomers ranging from 16-mers to 30-mers present, with a preference of even- (darker tone) over odd-stoichiometries (lighter tone). Protein samples (50 μM) were prepared in 200 mM NH_4OAc (pH 6.8) for the MS experiments.

Fig. 4: NTR αB-crystallin mutants are less thermostable and display differences in local structure compared to WT αB-crystallin. **a** Proteins (10 μM in 10 mM PB, pH 7.4) were incubated at room temperature for 30 min. Far UV-CD spectra were obtained and the results shown are representative of two independent experiments and spectra were

normalised to protein concentration. All variants, with the exception of S59A, exhibited greater negative ellipticity than αB-crystallin WT. The 54-60 inversion mutant exhibited the greatest negative ellipticity compared to WT. **b** Thermal denaturation curves of αB-crystallin mutants (50 µM in 50 mM PB, pH 7.4). The change in average particle size (Z-average) was measured by DLS with increasing temperature (ramp rate 2.5 °C per 15 min). **c** Intrinsic tryptophan fluorescence reveals differences in tertiary structure of some αB-crystallin variants, whereby the R56S/S59R and S59K αB-crystallin mutants have greater tryptophan fluorescence emission compared to WT. **d** bis-ANS fluorescence of αB-crystallin variants reveal that mutations results in decreased hydrophobic exposure compared to WT. Proteins (20 µM) for intrinsic tryptophan and bis-ANS fluorescence studies were incubated in 50 mM PB (pH 7.4) at room temperature for 15 min prior to measurement. Spectra in c and d were normalised to protein concentration and results shown are representative of two independent experiments.

Fig. 5: The ability of the NTR αB-crystallin mutants to inhibit the amorphous and fibrillar aggregation of insulin and α-synuclein. a The fibrillar aggregation of α-synuclein (10% seed relative to α-synuclein monomer concentration) was measured by the change in ThT fluorescence emission at 490 nm (excitation at 440 nm). All αB-crystallin variants showed no significant difference in their ability to inhibit α-synuclein seeded aggregation. **b** Inhibition of the reduction-induced amorphous aggregation of insulin was monitored by the change in light scatter at 340 nm. The 54-60 invert mutant showed a significant decrease in the ability to inhibit insulin aggregation at various stoichiometric ratios compared to WT αB-crystallin. Amorphous and fibrillar aggregation assays were performed in 50 mM PB (pH 7.4) at 37 °C. Data in a and b are mean ± SEM (n = 3) (*$p < 0.05$; **$p < 0.01$).

Figures

Fig 1

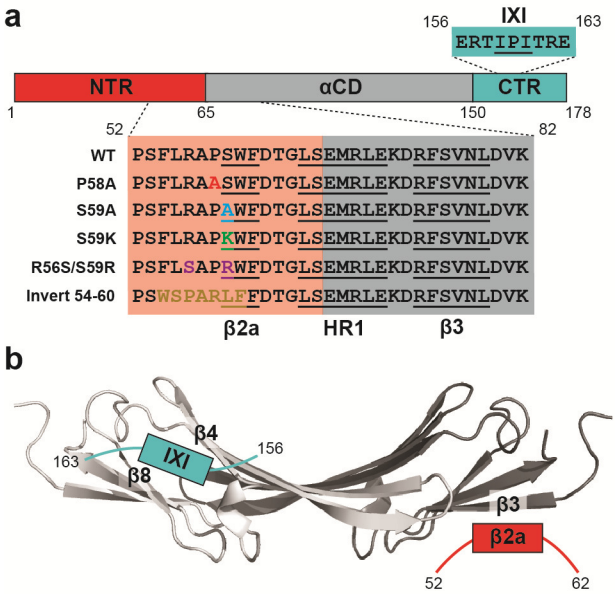

Fig 2

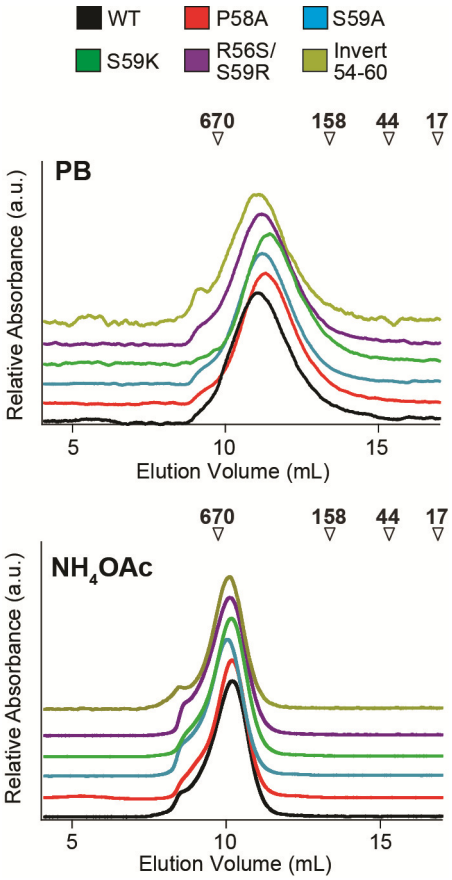
WT
P58A
S59A
S59K
R56S/ S59R
Invert 54-60
670
158
44
17
PB
Relative Absorbance (a.u.)
5
10
15
Elution Volume (mL)
670
158
44
17
NH4OAc
Relative Absorbance (a.u.)
5
10
15
Elution Volume (mL)

Fig 3

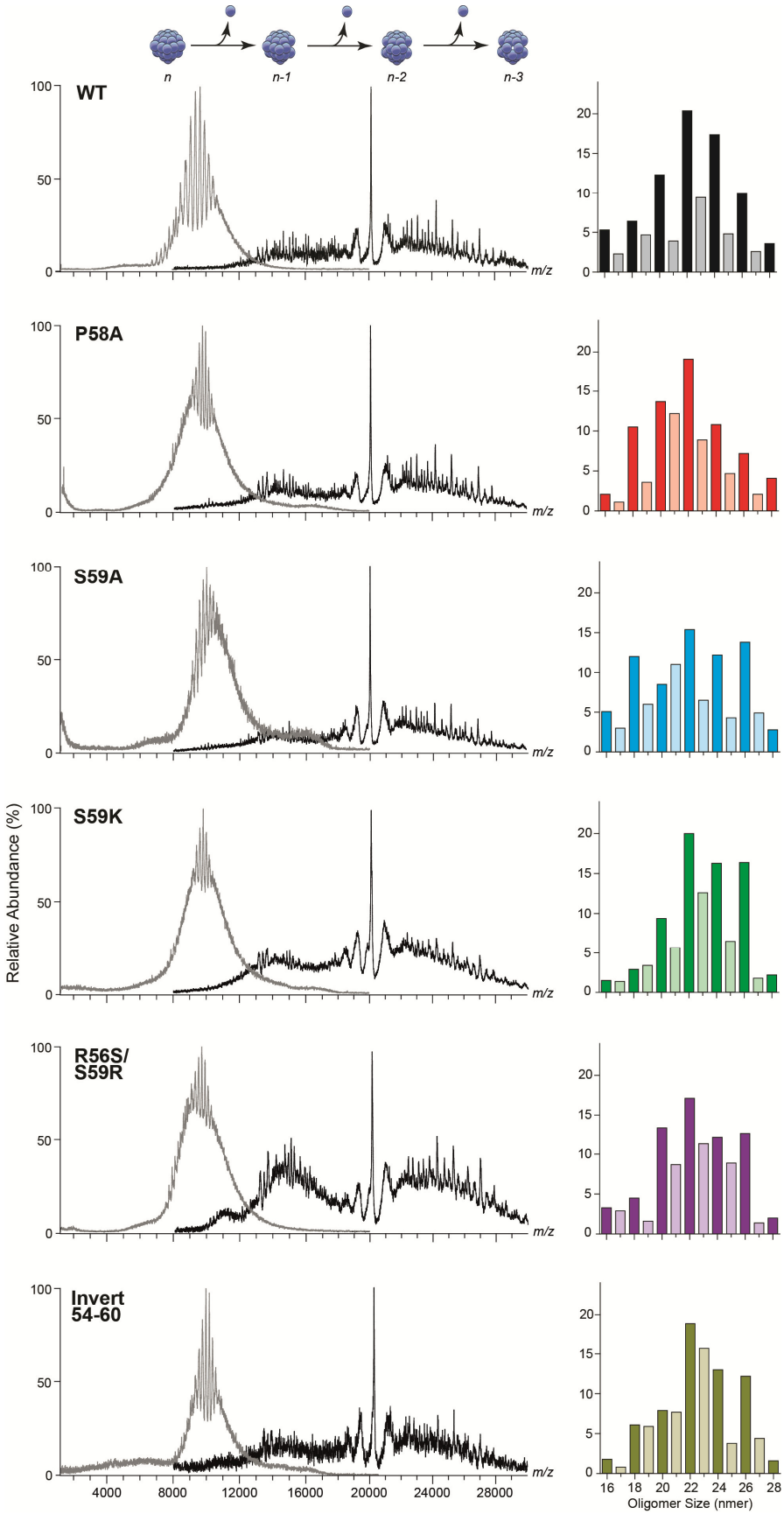
n
n-1
n-2
n-3
WT
P58A
S59A
S59K
R56S/
S59R
Invert
54-60
Relative Abundance (%)
m/z
4000
8000
12000
16000
20000
24000
28000
16
18
20
22
24
26
28
Oligomer Size (nmer)

Fig 4

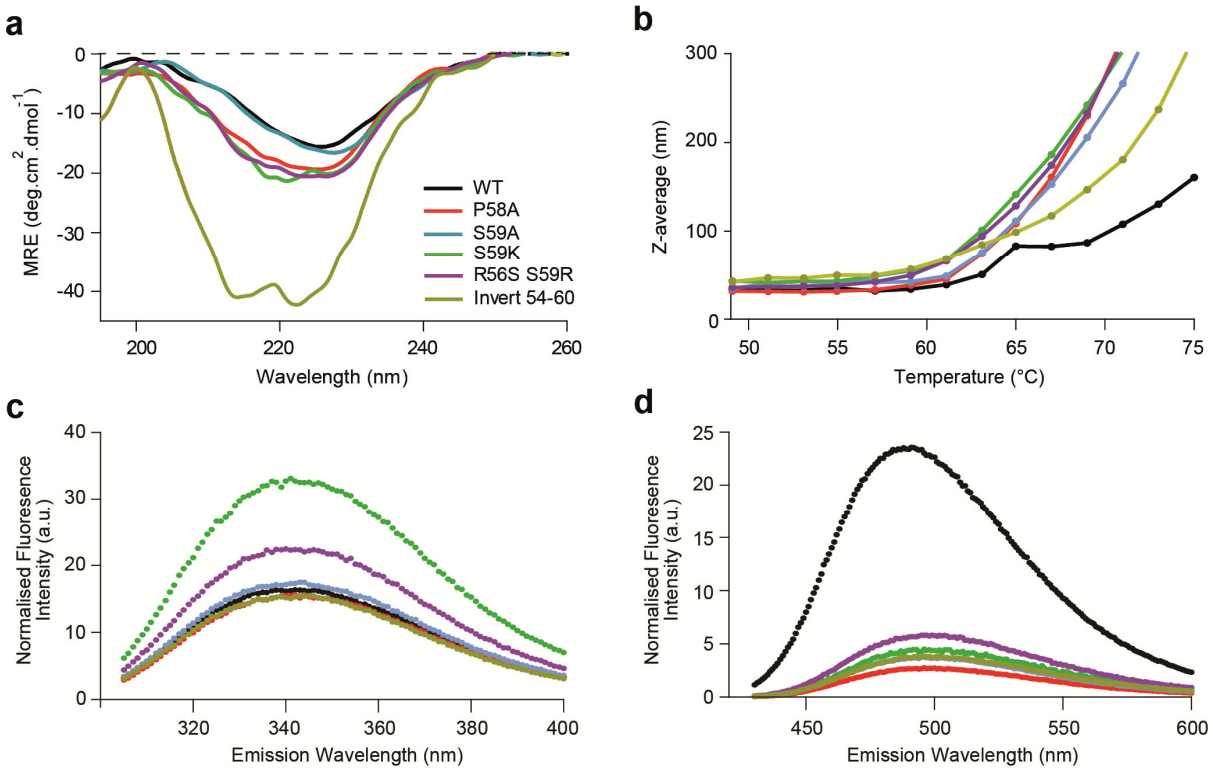
a
MRE (deg.cm^2.dmol^{-1})
0
-10
-20
-30
-40
200
220
240
260
Wavelength (nm)
WT
P58A
S59A
S59K
R56S S59R
Invert 54-60
b
Z-average (nm)
300
200
100
0
50
55
60
65
70
75
Temperature (°C)
c
Normalised Fluoresence Intensity (a.u.)
40
30
20
10
0
320
340
360
380
400
Emission Wavelength (nm)
d
Normalised Fluoresence Intensity (a.u.)
25
20
15
10
5
0
450
500
550
600
Emission Wavelength (nm)

Fig 5

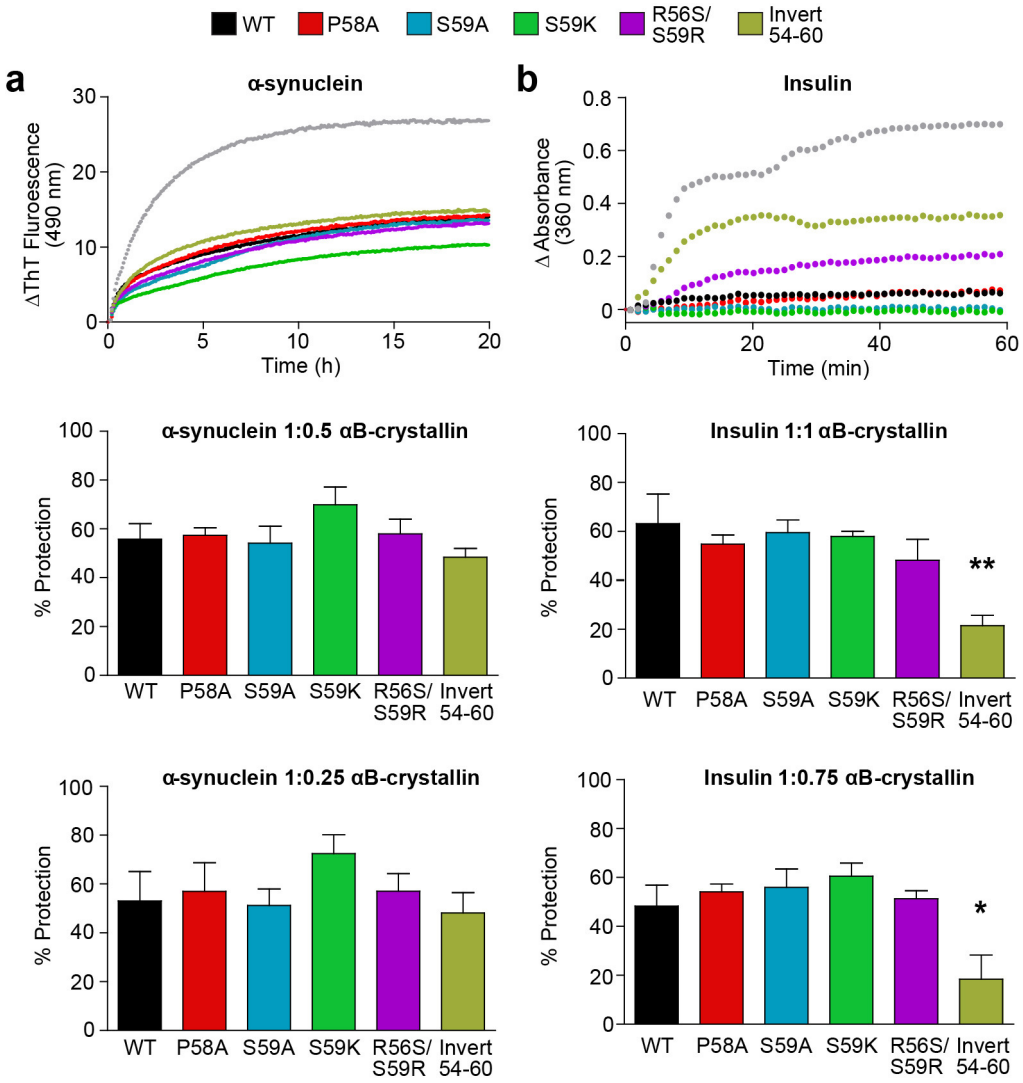
WT
P58A
S59A
S59K
R56S/ S59R
Invert 54-60
a
α-synuclein
ΔThT Fluroescence (490 nm)
Time (h)
b
Insulin
Δ Absorbance (360 nm)
Time (min)
α-synuclein 1:0.5 αB-crystallin
% Protection
Insulin 1:1 αB-crystallin
**
α-synuclein 1:0.25 αB-crystallin
Insulin 1:0.75 αB-crystallin
*

Supporting Information for:

The influence of the N-terminal region proximal to the core domain on the assembly and chaperone activity of αB-crystallin

Blagojce Jovcevski[1], J. Andrew Aquilina[1], Justin L. P. Benesch[2] and Heath Ecroyd[1†]

[1]*Illawarra Health and Medical Research Institute and School of Biological Sciences, University of Wollongong, Wollongong, New South Wales 2522, Australia*

[2]*Department of Chemistry, Physical and Theoretical Chemistry Laboratory, South Parks Road, Oxford OX1 3QZ, United Kingdom*

[†]Correspondence to: heathe@uow.edu.au, +61-2-4221-3443

Supporting Figures

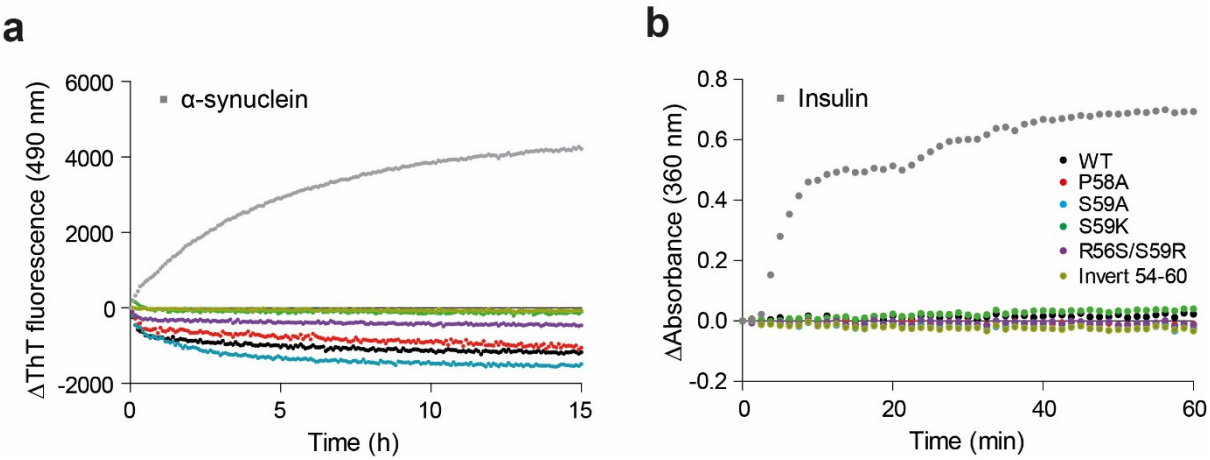

Fig. S1: The aggregation propensity of the NTR αB-crystallin mutants in the absence of fibrillar and amorphous aggregation-prone proteins. a In the absence of α-synuclein (10% w/w seed relative to α-synuclein monomer) there was no observable increase in ThT fluorescence at 490 nm, including when the αB-crystallin mutants (25 µM) were incubated alone. Amorphous and fibrillar aggregation assays were performed in 50 mM PB (pH 7.4) at 37 °C. **b** In the absence of insulin there was no observable increase in light scatter at 360 nm, including when the αB-crystallin mutants (75 µM) were incubated alone.